The Ductility of HAYNES® 242™ Alloy as a Function of Temperature, Strain Rate and Environment

Stephen D. Antolovich
Professor of Mechanical and Materials Engineering
Washington State University
Pullman, WA 99164-2920

Dwaine L. Klarstrom
Manager of Product Research and Development
Haynes International
1020 West Park Ave.
POB 9013
Kokomo, Indiana 46904-9013

John F. Radavich
President
Micro-Met Laboratories
209 North Street
West Lafayette, IN 47906

Abstract

HAYNES 242 is an alloy that is used when good combinations of strength, toughness and corrosion resistance are required. Since it is intended to be used for long time applications, the effects of temperature, time of exposure, and strain rate are all important factors that must be considered. In this study, the effects of prior exposure, temperature and strain rate were investigated as to their effects on mechanical properties such as yield strength (YS), ultimate tensile strength (UTS), and ductility (%RA). It is shown that the ductility and UTS increase with increasing strain rate when tested in air, in contrast to what is usually expected. When tested in vacuum, the ductility decreased with increasing strain rate in accord with usual observations. These contrasting behaviours are interpreted in terms of an environmental effect which causes changes in the fracture mechanism as well as the properties. It is noted that while there is an environmental effect, the absolute values of ductility remain very high making this material suitable for applications where long-term exposure and impact loading are considerations.

I. Introduction

HAYNES 242 alloy has an excellent combination of mechanical and physical properties and finds application at high temperatures in gas turbine seal rings where a good combination of ductility, strength, toughness, and low coefficient of thermal expansion is important [1]. Deformation has been determined in the past to occur through complex mechanisms including dislocation glide and twinning in a matrix containing very fine, ordered coherent $Ni_2(Mo,Cr)$ domains [2-6]. The object of this study was to determine the effects of temperature, strain rate, environment and prior exposure at high temperature on the strength and ductility of this important commercial alloy.

II. Experimental Procedure

A. Material

The material used in this investigation was HAYNES 242 Alloy whose nominal composition (wt %) is:

Ni [bal], Mo [25], Cr [8], Co [2.5 max], Mn [0.80 max], Si [0.80 max], Al [0.50 max], C [0.03 max], B [0.006 max], Cu [0.50 max] .

The material tested in this program was taken from heat 8422-3-7566 in the form of 12.7mm (0.5 inch) thick plate. Specimens were aged in air for either 24h or 1000h at 649C (1200F) after annealing in order to simulate potential service conditions.

Superalloys 2000
Edited by T.M. Pollock, R.D. Kissinger, R.R. Bowman, K.A. Green, M. McLean, S. Olson, and J.J. Schirra
TMS (The Minerals, Metals & Materials Society), 2000

B. Tensile Testing

Specimens were fabricated in the form of standard ASTM specimens with a 6.35 mm diameter and a 35.6 mm gage length. Tests were carried out at 427C and 649C (800F and 1200F) using nominal strain rates of 0.5, 5.0, and 50%/min (in one case the strain rate was 500%/min). Testing was done in air at 427C and 649C (800F and 1200F) and in vacuum at 649C (1200F). The vacuum was about 0.1×10^{-5} torr. The specimens tested in air had an extensometer directly attached and the strain rate could be controlled directly. The specimens tested in vacuum did not have an extensometer attached and the strain was computed from the crosshead displacement. Since there is considerable deflection in the load train, the crosshead displacement does not represent the displacement in the specimen. The strain rate was controlled using a pacing technique. Since the load/displacement records were in terms of cross head displacement, they had to be corrected to reflect actual specimen strain. At low loads, the displacement was made up entirely of elastic deflection of the specimen and elastic deflection of the machine. However, Young's Modulus of the HAYNES 242 alloy was known and the deflection of the specimen could be subtracted from the total elastic deflection to yield machine deflection. Since the machine deflection will *always* track linearly with load, a curve for machine deflection v. load could be established. This then permitted the machine deflection to be subtracted from the total deflection at *any* load. Thus actual engineering stress/strain curves could be constructed. The stress/strain curves for all of the vacuum tested materials were determined in this way. A partial check of the validity of the technique is to note the measured longitudinal strain and to compare it with the strain computed from the stress/strain curves determined as described above. In all cases the agreement was quite good.

C. Optical Microscopy SEM Examinations

Specimens were examined via optical metallography and SEM to gain some insight into the microstructure, fracture features and the mechanisms of failure. Standard metallography and SEM procedures were used.

D. TEM Examination

Representative specimens were examined via TEM to determine if there were substantial changes in the deformation mode, which could account for the ductility changes that were observed. Foils were taken near the fracture surfaces (for the most part) and were polished using standard techniques. A 200 kV TEM with analytical capability was used.

III. Results and Discussion

A. Tensile Test Results

The results of the tensile tests are tabulated in Tables I and II where yield strength, tensile strength, elongation, and per cent reduction in area are given.

Table I - Tensile Test Results for All Specimens Tested at 649C Air and Vacuum

Spec ID	Strain Rate (%/min)	0.2% YS (MPa)	UTS (MPa)	Elong (%)	RA (%)	Comments Vac (Torr)
Aged at 649C for 24 hrs - Alloy 8422-3-7566						
24-12	0.5	630.0	928.9	14.0	22.0	
24-3-V	0.5	626.5	1043.0	47.0	70.0	0.1×10^{-5}
24-4-V	0.5	619.5	1043.0	44.0	73.0	0.1×10^{-5}
24-4	5.0	574.0	994.0	20.0	22.0	
24-10	5.0	581.0	1001.0	19.0	26.0	
24-1-V *	5.0	612.5	1065.0	25*	23*	1×10^{-5}
24-2-V	5.0	605.5	1064.0	36.0	64.0	0.1×10^{-5}
24-5-V	5.0	602.0	1071.0	37.0	61.0	0.1×10^{-5}
24-6-V	50.0	595.0	1036.0	33.0	58.0	0.1×10^{-5}
24-13-V	50.0	595.0	1057.0	34.0	54.0	0.1×10^{-5}
24-2	50.0	651.0	1064.0	31.0	49.0	
24-1	50.0	591.5	1057.0	33.0	53.0	
24-9	50.0	574.0	1050.0	35.0	58.0	
24-3	500.0	640.5	1043.0	32.0	56.0	
Aged at 649C for 1000 hrs - Alloy 8422-3-7566						
1000-10	0.5	714.0	861.0	3.0	2.6	Fail in thrd
1000-11	0.5	721.0	903.0	3.7	3.5	Fail in thrd
1000-13-V	0.5	728.0	1099.0	43.0	69.0	0.1×10^{-5}
1000-4-V	0.5	714.0	1141.0	34.0	60.0	0.1×10^{-5}
1000-3	5.0	728.0	1015.0	9.0	16.0	
1000-4	5.0	721.0	994.0	9.5	17.0	
1000-12-V	5.0	728.0	1134.0	30.0	56.0	0.1×10^{-5}
1000-3-V	5.0	707.0	1148.0	29.0	54.0	0.1×10^{-5}
1000-2	50.0	704.9	1092.7	18.0	24.0	
1000-1	50.0	702.8	1117.9	22.0	30.0	
1000-1-V	50.0	686.0	1127.0	27.0	55.0	2.0×10^{-5}
1000-2-V	50.0	689.5	1120.0	26.0	50.0	0.1×10^{-5}

V = tested in vacuum. Vacuum level is indicated in torr
* = ductility data not valid - stopped before failure -pulled out of adapter

The results in Table I show that there is a large effect of strain rate, environment and aging time on ductility with less of an effect of these variables on the yield and ultimate strengths. Similar conclusions can be drawn about the air testing carried out at 427C as seen in Table II.

Table II - Tensile Test Results for 427C - Air Only

Spec ID	Strain Rate (%/min)	0.2% YS (MPa)	UTS (MPa)	Elong (%)	RA (%)
Aged at 649C for 24 hrs - Alloy 8422-3-7566					
24-11	0.5	650.3	1214.5	38.0	44
24-8	5.0	651.0	1190.0	39.0	48
24-7	5.0	651.0	1183.0	38.0	49
24-6	50.0	654.5	1155.0	41.0	46
24-5	50.0	658.0	1169.0	39.0	51
Aged at 649C for 1000 hrs - Alloy 8422-3-7566					
1000-9	0.5	728.0	1295.0	29.0	47
1000-7	5.0	770.0	1295.0	31.0	42
1000-8	5.0	777.0	1281.0	31.0	43
1000-6	50.0	753.2	1257.2	31.0	42
1000-5	50.0	758.9	1242.5	29.0	43

A typical stress/strain curve is shown in Fig. 1.

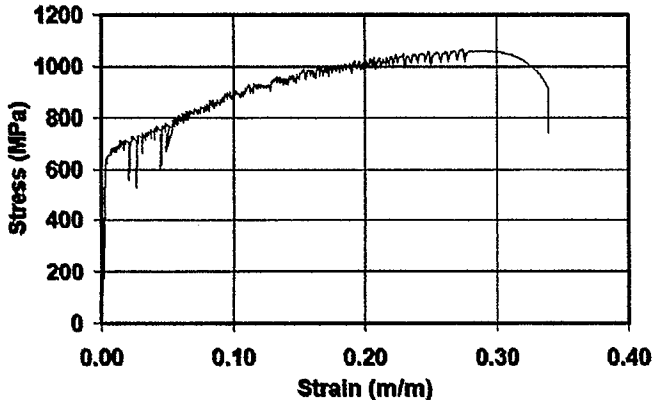

Fig.1. Stress/strain curve for specimen 24-2. Aged 24 hrs at 649C and tested at 649C and 50%/min in air.

The features seen in Fig. 1 were similar for air and vacuum. The serrations on the stress/strain curve are associated with either dislocation "bursts" or deformation by twinning. It has been shown in the literature that deformation occurs by both mechanisms. [2-5]. It is not likely that there is a strain aging effect here since the drops are too large and the range of conditions for which this behavior are observed are too extensive for such a mechanism to be operating. A stress strain curve for specimen 1000-V-4, tested and aged under different conditions is shown in Fig. 2. Specimens tested under these conditions also exhibited serrated stress strain curves. However, due to limitations of the equipment, testing was done in cross head control and machine deflection was subtracted out analytically. The test method and the data reduction procedure both operated to artificially reduce the appearance of the serrations.

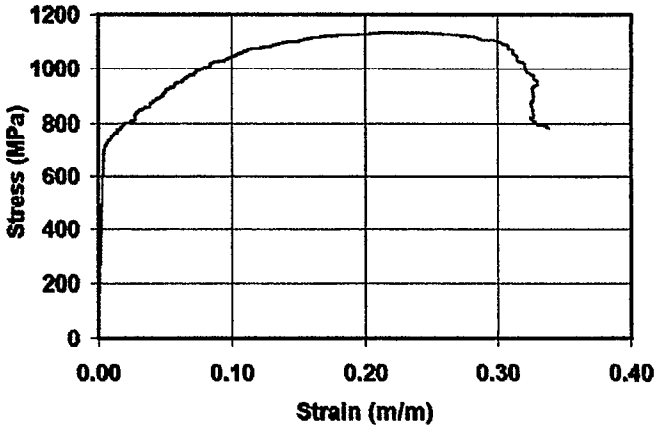

Fig. 2 . Stress strain curve for specimen 1000-V-4. Aged 1000 hrs at 649 C and tested at 649C at 0.5%/min

For completeness, a stress strain curve for specimen 1000-7, aged 1000 hrs at 649C and tested at 427C in air is shown in Fig. 3.

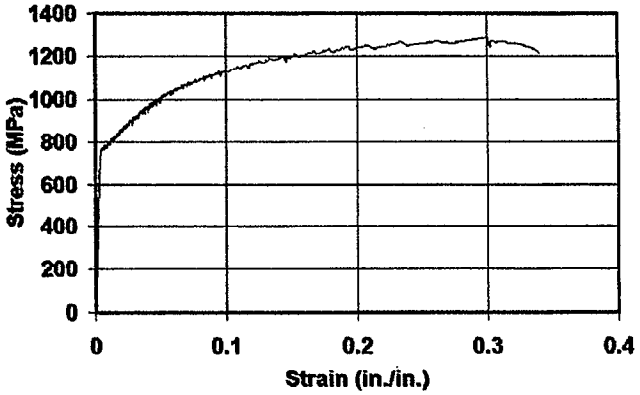

Fig. 3. Stress strain curve for specimen 1000-7. Aged 1000 hrs at 649C and tested at 427C at 5%/min in air.

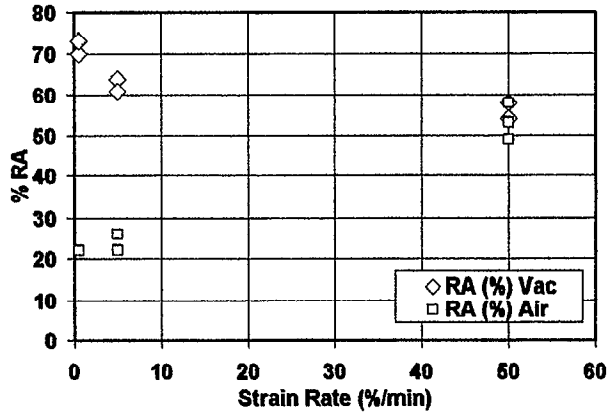

Fig. 4. % RA v strain rate for material aged for 24 hrs at 649C and tested in air & vacuum at 649C.

Figure 4 (24 hr age material) demonstrates that the ductility in vacuum is significantly higher than it is in air at the low strain rates. It is significant that:

1. ductility decreases with increasing strain rate for the vacuum tests , an expected result while,
2. ductility *increases* with strain rate in air, a rather uncommon and unexpected result.
3. the ductilities for both conditions converge at a strain rate of about 50%/min.

Similar behavior is observed in Fig. 5 for material that was aged for 1000 hrs at 649C and tested at 649C. The difference between these conditions is that the ductilities at a given strain rate are significantly lower and convergence appears to be shifted to higher strain rates (with a lower ductility). The lower ductility may be understood in terms of a larger embrittled zone. Reasons for the shift to convergence at higher strain rates is less intuitive.

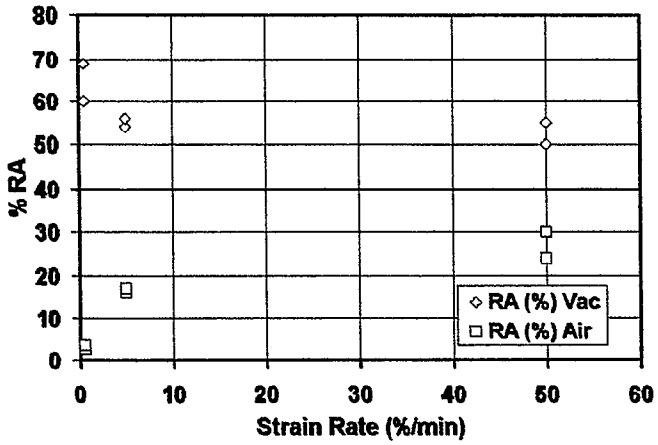

Fig. 5. % RA v strain rate for material aged for 1000 hrs at 649C and tested in air or vacuum at 649C

The ductility at 427C for ageing at 649C either 24 or 1000 hrs is shown in Fig. 6. In this figure it can be seen that the ductility is relatively constant (somewhat lower for the longer term age).

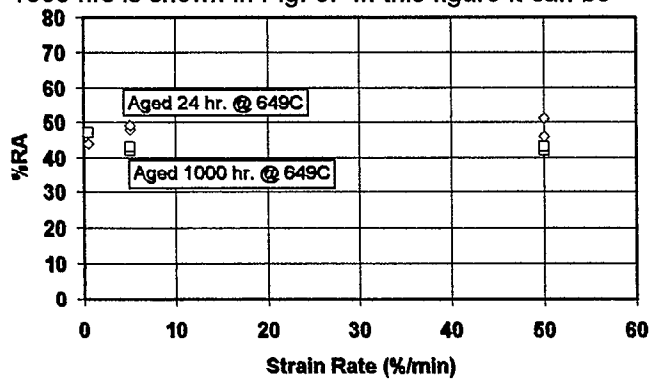

Fig. 6. % RA v strain rate for material aged for 24 or 1000 hrs at 649C and tested in air at 427C.

Note that the data scatter is small in all cases making it possible to draw unambiguous conclusions.

Figures 7-9 shows the strength properties as a function of strain rate. Here we see that the yield strength for both air and vacuum are virtually identical while there is a modest increase of the UTS for the material tested in vacuum over that tested in air at the low and intermediate rates.

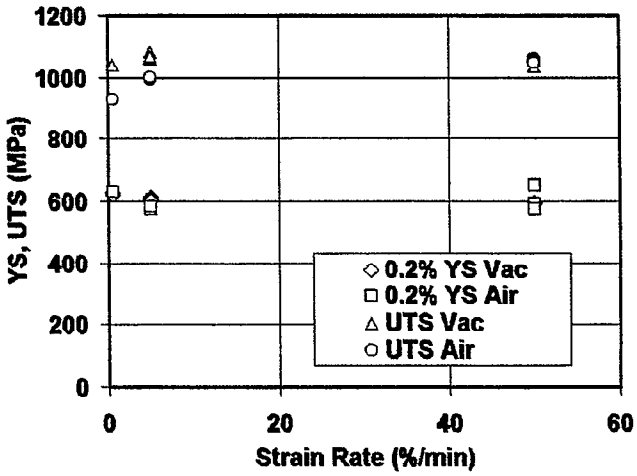

Fig. 7. Yield and tensile strength v strain rate for material aged for 24hrs at 649C and tested in air or vacuum at 649C.

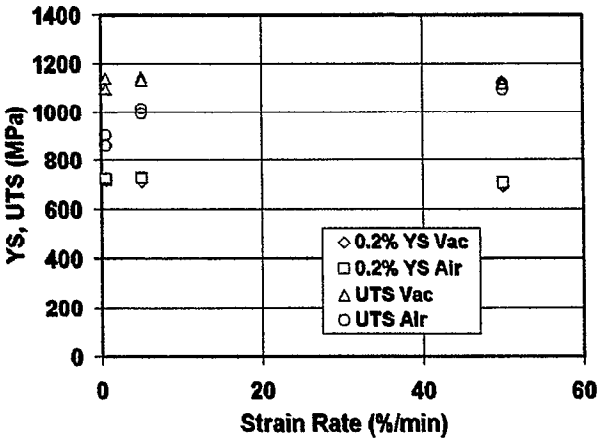

Fig. 8. Yield and tensile strength v strain rate for material aged for 1000 hrs at 649C and tested in air or vacuum at 649C.

All of these observations are fully consistent with an environmental effect. The increased ductility of the vacuum-tested material over the air-tested material at

649C can be understood on the basis of reduced ductility or toughness in air. In other words, in terms

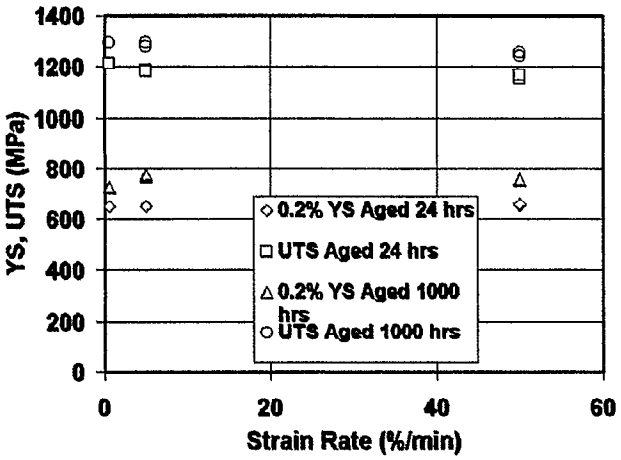

Fig. 9. Yield and tensile strength v strain rate for material aged for 24 or 1000 hrs at 649C and tested in air at 427C.

of an environmental effect. However, the ductility in air *increases* with strain rate (an unusual but not unique effect) because with increasing strain rate the time for a deleterious environmental effect (e.g. diffusion of oxygen) is reduced. Thus even though the intrinsic ductility would be expected to decrease (as seen in the vacuum tests) this is offset by the effect of the environment. The decrease in ductility with increasing strain rate observed in the vacuum tests is simply the usual trend observed in most metallic alloys. The strength data supports this argument as well. The yield strength is not much affected by environment since it is a measure of the first dislocation movement. Hence it is not surprising to see the vacuum and air yield strengths essentially the same. However, the UTS is affected by environment; during the time it takes to reach the UTS there is time for environmental interactions and hence a reduced toughness which is reflected in a lower UTS for the air tested material. It is well known that increased strain rate will increase the flow stress. Thus if there were an environmental effect we would expect to see similar yield strengths, higher tensile strengths for the vacuum tested material and increasing tensile strengths for each with convergence to a common value at some point. To repeat, this convergence is seen at a strain rate of about 50%/min. The environmental explanation fits very well with the specimens tested in this program.

The same trends are observed for the material that was aged for 1000 hrs. before testing except that the elongation and %RA did not converge at 50%/min. while the yield and ultimate strengths did converge. The ductility was reduced only modestly for the vacuum tested material compared to the material which was aged for 24 hrs. This observation may be taken as an indication that extensive ageing doesn't significantly affect the *intrinsic* ductility that is measured in the vacuum tests. The ductility for the air tests showed a very large drop from the 24 hr. age, especially at the lowest strain rates. This would indicate that there is a strong environmental effect but that there may be significant structural changes when aged for 1000 hrs. which promote even more environmental damage in the course of the test. This would seem to follow from the fact that independent of how the testing was done, all starting material was aged under similar conditions in air prior to machining samples from the interior. These results indicate that there is a dynamic environmental effect associated with the deformation mode which may be influenced by structural changes during aging. Such a conclusion is strengthened by considering the yield and ultimate tensile strength results. As the ageing time is increased from 24 to 1000 hrs, there is a small but definite increase in the yield strength and a smaller increase in the tensile strength as seen in comparing the results in Figs. 7 and 8. These strength differences are consistent with modest changes in the underlying microstructure.

Testing at 427C did not reveal any rate effects, either on ductility or strength, as can be seen in Figs. 6 and 9. There were, however, modest ageing effects; the ductility of the material aged for 1000 hrs was modestly lower than that aged for 24 hrs and the strengths for the 1000 hr age were higher. These observations are fully consistent with the preceding comments on structural changes and the lack of an environmental effect at 427C. The absence of a rate effect can be understood in terms of an elementary diffusional model which follows the Arrhenius relationship and in which the activation energy is assumed to be unaffected by stress. These assumptions result in an equation of the form:

$$\frac{1}{\tau} = \mathbf{A}\exp\left(-\frac{\mathbf{Q}}{\mathbf{RT}}\right) \qquad \ldots (1)$$

where τ = characteristic process time (sec)
Q = activation energy (cal/mol)
R = gas constant (1.987 cal/mol-K)
T = temperature (K)

If an activation energy of 50,000 cal/mol is assumed (reasonable for many processes in these kinds of alloys including oxygen diffusion) then the ratio of the characteristic times at 427C (700K) and 649C (922K) is calculated to be about 5740. This means that a

process that requires 0.1 sec at 649C, say, will require just about 10 minutes at 427C. Given this large difference it is not surprising that the rate effect is masked at the lower test temperature. Another way of looking at this is that the material is practically impervious to environmental degradation at temperatures of 427C and lower.

B. Optical Metallography

The microstructure after annealing is shown in Fig. 10 and after ageing in Fig. 11. It can be seen that the microstructure contains intermediate sized grains, twins, and stringers. The stringers and grain boundary precipitates have been identified as carbides and μ phase. The stringers and precipitates hold the grain size down and determine the grain size between them.

Fig. 10. Optical micrograph of sample annealed at 1066C for 30 min. and water quenched.

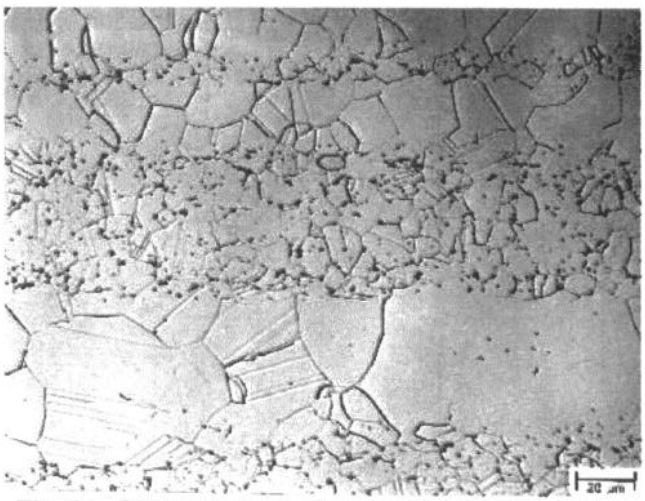

Fig. 11. Microstructure of material annealed and aged for 1000 hrs at 649C.

The effect of the precipitates is clearly seen in Fig. 11.

The grains are very large where the precipitate density is low and very small where the precipitate density is high. This is an excellent practical example of Zener pinning.

C. Scanning Electron Microscopy (SEM)

Specimens were examined via SEM to see if there were any significant differences in the fracture features as a function of pre-treatment or testing mode. In general, specimens tested in air at low rates and high temperatures tended to show secondary cracking (i.e. cracking on the side surfaces of the specimen) and significant areas in which the cracking mode was intergranular. A typical SEM micrograph of the surface of a specimen tested in air is shown in Fig. 12.

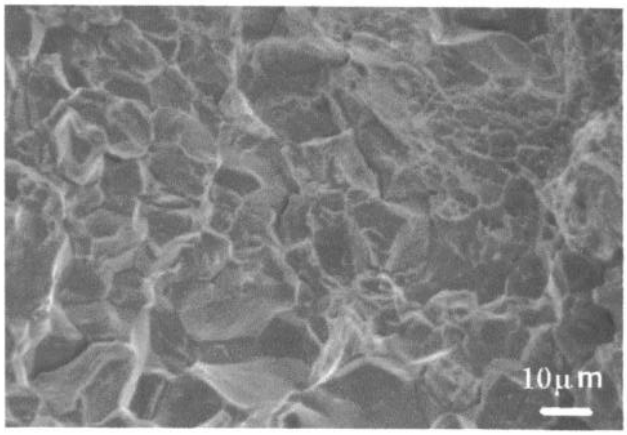

Fig. 12. Fracture surface of specimen tested in air at 649C and 0.5%/min. Note the large area of intergranular fracture along with some ductile dimpling.

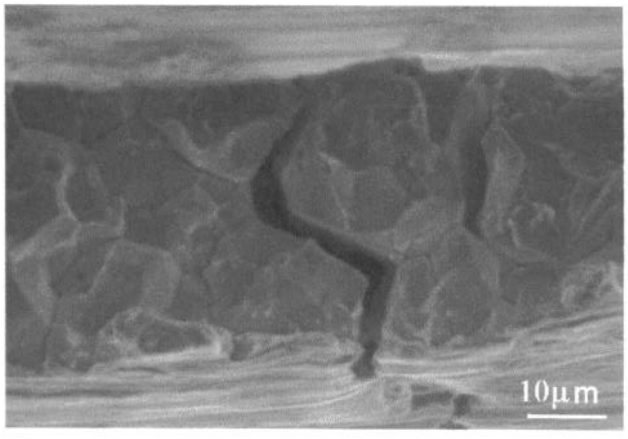

Fig. 13. Intergranular cracking on the side of same specimen as in Fig. 12.

The initiation of intergranular fracture on the side of the specimen is seen clearly in Fig. 13 for the same

specimen. Features similar to those seen in Figs. 12 and 13 were seen for the air tested specimens with the amount of intergranular cracking decreasing as the strain rate was increased. However, for specimens tested in vacuum, the situation was completely different. The fracture features of a vacuum tested specimen are seen in Figs. 14 and 15.

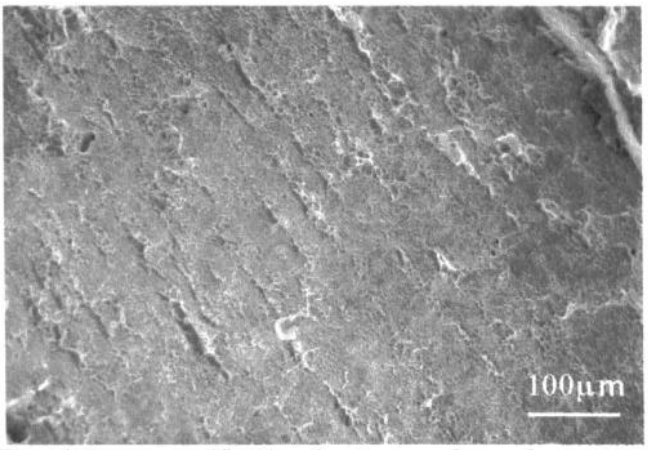

Fig.14. Low magnification fracture surface of specimen tested in vacuum at 649C and at 0.5%/min. Note the aligned stringers.

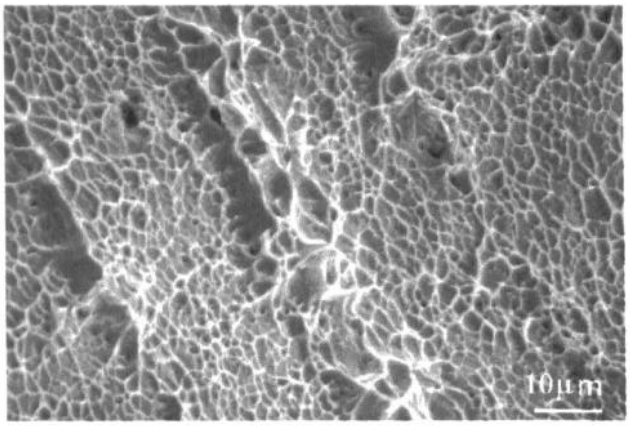

Fig. 15. Higher magnification of fracture surface shown in Fig. 14. Note the shallow ductile dimples and effect of stringers.

The fracture surfaces did not exhibit any intergranular cracking nor were there any significant cracks on the sides of the specimen. Furthermore, the great majority of the fracture surface consisted of "ductile dimples" albeit of a rather shallow nature. In short, under the same test conditions, the fracture features are essentially ductile in vacuum and brittle in air.

Figure 14 shows macroscopic aligned "stringers" features which were commonly seen on fracture surfaces of vacuum tested and air tested materials. In these regions, we have demonstrated that there are large particles whose composition is close to the overall-composition. When these were analyzed in the TEM it was found that they were essentially large precipitate particles (with perhaps some carbides). This is evidence of a macroscopic processing effect which may have to do with solidification and subsequent mechanical working, much like banding in steels. These regions are involved in the fracture process. However, their role in crack initiation and in providing easy paths for rapid diffusion of a degrading species is not clear.

These observations are entirely consistent with the tensile test results where the macroscopic ductility was greater for the vacuum tests than for the air tests. The grain boundaries of some specimens which were given a prolonged thermal exposure were examined to see if the environmental effect could be explained by grain boundary precipitation effects. In no case that was examined was it possible to find any evidence of enhanced grain boundary precipitation of carbides or μ phase. We thus tentatively conclude that the environmental sensitivity is not a result of the formation of a new, deleterious phase.

D. Transmission Electron Microscopy (TEM)

Specimens typical of all of the conditions tested were examined by TEM in a effort to determine if there were
significant differences in the deformation mode with strain rate, temperature, and aging time. The major result was that the deformation mode was essentially independent of environment (air or vacuum), temperature, strain rate or aging conditions over the range of conditions investigated in this study. Representative TEM micrographs are shown in Figs. 16-20. Figure 16, taken from specimen 24-5V (24 hr age and tested at 5%/min in vacuum at 649C) shows a deformation substructure that was generally characteristic of all conditions studied; planar deformation with a high density of slip bands and/or twins. Figure 17 is a dark field image taken from the same region as Fig. 16. This image was formed using a beam diffracted from the coherent precipitates and demonstrates unambiguously that the precipitates are being sheared (the local order is destroyed by shearing and the deformation band shows up dark while the precipitates outside of the band are bright). Figure 18 shows the deformation substructure of specimen 1000-9 (1000 hr age and tested at 0.5%/min in air at 427C). It has a structure similar to that seen in Fig. 16 although the ageing and test conditions were quite different. Figure 19 is a dark field image of the
region showed in Fig. 18. Shearing of the precipitates is again observed. In addition, it is clear that ageing

for 1000 hrs significantly increases the precipitate size.

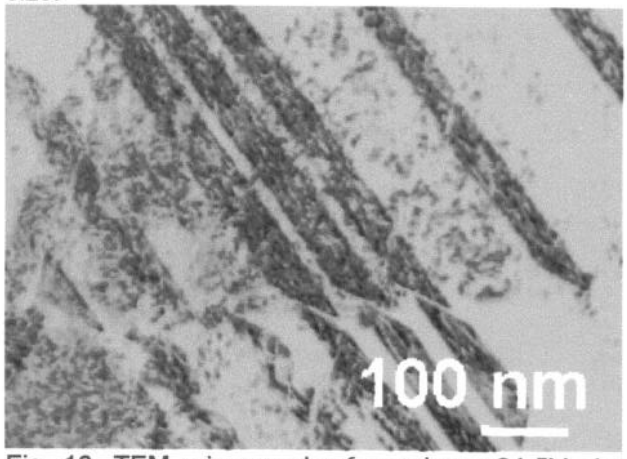

Fig. 16. TEM micrograph of specimen 24-5V. Aged 24 hrs at 649C and tested at 5%/min in vacuum at 649C. Note planar deformation bands.

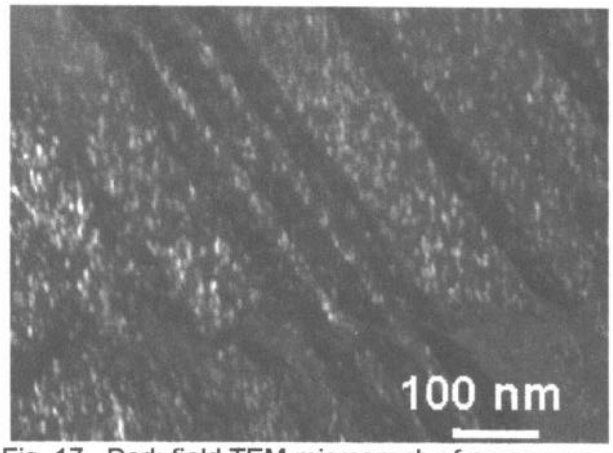

Fig. 17. Dark field TEM micrograph of same area as seen in Fig. 16. Note the fine precipitates and strong evidence of precipitate shearing.

It is well known that as long as precipitate shearing remains operative, the strength increases with increasing precipitate size. Thus the increase in strength that was observed with increased ageing time is completely consistent with the microstructure. This increase in strength is also consistent with a reduction in ductility, especially in air. The higher stresses that can develop in the long-term aged material coupled with environmental ingress (which is a zone of weakness) gives rise to a reduction in the toughness or ductility. These ideas have been verified for many superalloys by one of the authors of this paper [7-15].

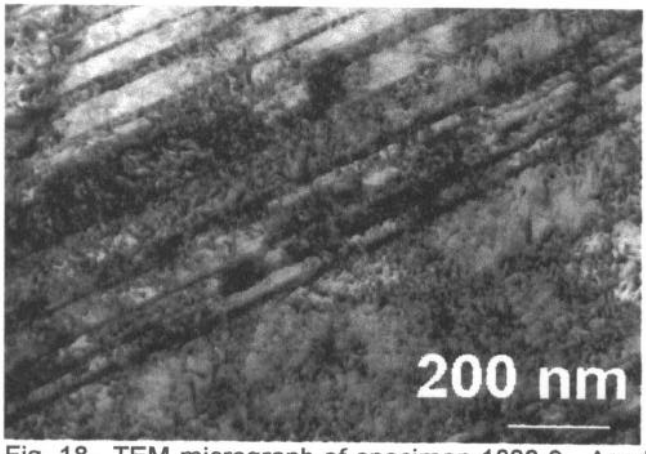

Fig. 18. TEM micrograph of specimen 1000-9. Aged 1000 hrs at 649C and tested at 0.5%/min in air at 427C. Planar deformation bands are again present.

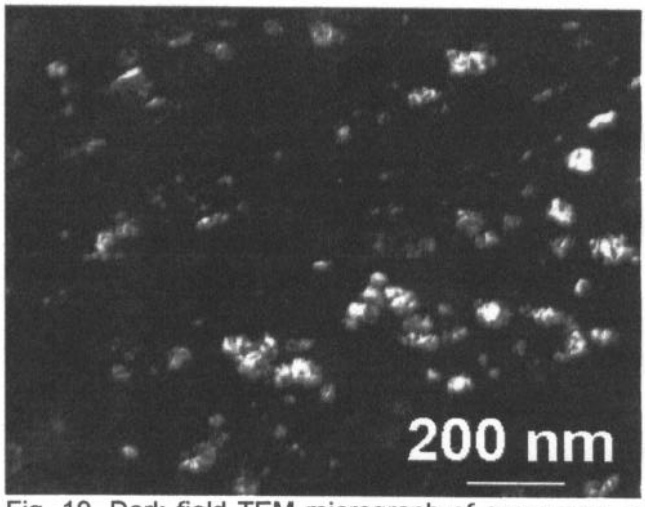

Fig. 19. Dark field TEM micrograph of same area as seen in Fig. 18. Note the significantly coarsened precipitates and precipitate shearing.

Figure 20 is a TEM micrograph taken from a low temperature/high rate test. Again planar deformation features, similar to those observed in all other specimens, are seen. Thus it appears as if *changes* in the deformation mode are not responsible for the drop in ductility. Deformation consisted of planar arrays of slip bands and twins (quasi twins to be precise). Both of these deformation modes would be expected to produce more sensitivity to environmental effects than wavy glide. The slip steps at the surface could break any protective film and could also provide energetically favorable sites for the dissociation of the damaging species.

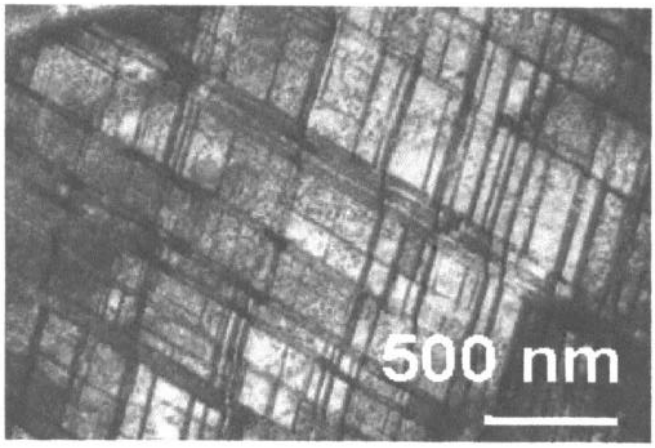

Fig. 20. TEM micrograph of specimen 1000-6. Aged 1000 hrs at 649C and tested at 50%/min in air at 427C. Planar deformation bands are again present.

The picture that develops is that at low rates the environment, aided by the planar deformation mode, has time to penetrate into the specimen and to reduce the ductility by what is probably a very complex mechanism involving changes in the interatomic bonding forces. As the strain rate increases, the time for environmental interactions is decreased and the behavior of the material approaches that characteristic of vacuum. Prolonged ageing causes a moderate decrease in the ductility through a precipitate coarsening mechanism. However, the fact that the ductility is high on an absolute basis and increases for impact loading in air implies that this alloy has a significant degree of damage tolerance and is suitable for many engineering applications.

IV. Summary and Conclusions

Based on the results of the experimental program the following conclusions can be drawn:

1. The ductility of this alloy is substantial for all temperatures, strain rates and prior exposures that were investigated.

2. The ductility in air increased with increasing strain rate while in vacuum it decreased. The ductilities for materials that were tested at 649C (1200F) in air and vacuum after exposure at 1000F for 24 hrs converged at a strain rate of about 50%/min.

3. The ductility for specimens aged for 1000 hrs at 649C (1200F) followed the same trends as for the 24 hr aged materials except that convergence was apparently shifted to higher strain rates.

4. The ductility at 427C (800F) was essentially independent of strain rate. This was explained on the basis of a thermally activated damage mechanism whose rate was calculated (assuming Arrhenius behavior and an activation energy of 50 [k-cal/mol]) to be reduced by several orders of magnitude at the low temperature.

5. Increasing the ageing time from 24 to 1000 hrs had the effect of increasing the precipitate size, increasing the strength and decreasing the ductility, all in accord with established physical metallurgy principles.

6. The fracture surfaces of those specimens tested in air exhibited a significant degree of intergranular cracking, especially at the lower strain rates.

7. The deformation substructure consisted of linear arrays of dislocations and/or twins.

8. The strength was generally lower in air than in vacuum for equivalent exposures, temperatures and strain rates.

9. The previous four conclusions are consistent with an environmental effect , similar to that observed in some other high temperature alloys.

10. The fact that the ductility is quite substantial and increases with increasing strain rate implies that this alloy is suitable for applications in which impact loads may be encountered.

References

1. S.K. Srivastava and G.Y. Lai: Paper presented at ASME Gas Turbine and Aeroengine Congress, Toronto (1989), Paper 89-GT-329.

2. S. Dymek, M. Dollar, and D.L. Klarstrom: Scripta Met., 10, (1991), 865-869, 1991.

3. M. Kumar and V.K. Vasudevan: Acta. Met., 44, (1996), 3575-3583.

4. M. Kumar and V.K. Vasudevan: Acta Met., 44, (1996), 4865-4880.

5. M. Kumar: Ph.D. Dissertation, University of Cincinnati, Cincinnati, OH, (1995)

6. S.K. Srivastava: Superalloys 1992, S.D. Antolovich, R.W. Stusrud, R.A. MacKay, D.L. Anton, T. Khan, R.D. Kissinger, D.L. Klarstrom eds., TMS, Warrendale, PA, (1992), 227-236.

7. Stephen D. Antolovich, P. Domas and J. L. Strudel: Met. Trans., vol. 10A, (1979),1859-1868.

8. Stephen D. Antolovich. S. Liu and R. Baur: Superalloys 1980, Tien, Wlodek, Gell and Maurer, eds. ASM, Metals Park, OH (1980), 605-615.

9. Stephen D. Antolovich, S. Liu and R. Baur: Met. Trans., vol. 12A, (1981),473-481.

10. Stephen D. Antolovich and N. Jayaraman: Fatigue: Environment and Temperature Effects, J. J. Burke and V. Weiss, eds., Plenum Press, NY, (1983),119-144.

11. Stephen D. Antolovich and J. E. Campbell: Superalloys Source Book, ASM, (1984),112-169.

12. B. A. Lerch, Stephen D. Antolovich and N. Jayaraman: Mat. Sci. and Engr., (1984),151-165.

13. Stephen D. Antolovich: Superalloy 718-Metallurgy and Applications, ed., E.A. Loria, TMS, Warrendale, Pennsylvania, (1989), 647-653.

14. Bruce F. Antolovich, Ashok Saxena, and Stephen D. Antolovich: Superalloys 1992, S.D. Antolovich, R.W. Stusrud, R.A. MacKay, D.L. Anton, T. Khan, R.D. Kissinger, D.L. Klarstrom eds., TMS, Warrendale, PA, (1992), 727-736.

15. M.P. Miller, D.L. McDowell, R.L.T. Oehmke, and S.D. Antolovich: Thermomechanical Fatigue Behavior of Materials, ASTM STP 1186, Ed. H. Sehitoglu, (1993), 35-49.